SI Appendix

Biosynthetic pathway toward carbohydrate-like moieties of alnumycins contains unusual steps for C–C bond formation and cleavage.

Terhi Oja[1], Karel D. Klika[2], Laura Appassamy[1], Jari Sinkkonen[2], Pekka Mäntsälä[1], Jarmo Niemi[1] & Mikko Metsä-Ketelä*[,1]

[1]Department of Biochemistry and Food Chemistry, University of Turku, FIN-20014 Turku, Finland

[2]Department of Chemistry, University of Turku, FIN-20014 Turku, Finland

*Corresponding author, e-mail: mikko.mk@gmail.com

Contents

S1. Supplementary Tables S1–S3 and Supplementary Figure S1

Supplementary Table S1. Incorporation of labeled D-ribose into alnumycin A (**1**, Supplementary Fig. S1) given as the relative increase of ^{13}C-edited ^{1}H signal intensity*. The values were obtained through feeding of [U-^{13}C] D-ribose to a) *S.* sp. CM020 vs. b) to *S. albus*/pAlnuori, and from the feeding of c) [1-^{13}C] D-ribose to *S. albus*/pAlnuori and d) [5-^{13}C] D-ribose to *S.* sp. CM020 (acquired as DEPT spectra). Positions of the ^{13}C -label within the dioxane unit are shown in red.

	a) U-^{13}C	b) U-^{13}C	c) 1-^{13}C	d) 5-^{13}C
Position		**Intensity ratio**		
1'	2.6	5.6	16.3	1
3'	2.8; 2.0	5.6; 4.4	2.0; 1.3	4.8
4'; 6'	2.3	4.9	2.6	1.8; 5.3
5'	2	1.8	4.4	1.2
1	1.3	1.9	2.5	1.4
4	1	1.5	2.7	3.9
5	1	1	1.2	3.9
7	1.2	1.1	1	1.3
11; 14	1.4	1.8	3.3	1.8; 4.4
11; 12	1.2	1.2	3	–; 1.4
13	1.2	1.3	2.7	4.1

*Representative results are shown. Various analytical procedures (e.g. addition of $Cr(acac)_3$ and different detection methods including ^{13}C, ^{13}C-edited ^{1}H and DEPT) were enacted in order to find the optimal conditions. The highest background incorporation levels into the polyketide backbone were consistently observed for *S.* sp CM020.

Supplementary Table S2. Incorporation of labeled D-ribose into alnumycin B (**4**, Fig. 1) given as the relative increase of ^{13}C-edited ^{1}H signal intensity* from the feeding of [U-^{13}C] D-ribose to a) *S. albus*/pAlnuoriΔ*aln3* vs. b) to *S. albus*/pAlnuori and from the feeding of c) [1-^{13}C] D-ribose to *S. albus*/pAlnuori and d) [5-^{13}C] D-ribose to *S.* sp. CM020. Positions of the ^{13}C -label within the dioxolane unit are shown in red.

	a) U-^{13}C	b) U-^{13}C	c) 1-^{13}C	d) 5-^{13}C
Position		**Intensity ratio**		
1'	4.7	6.1; 4.3	13.9; 15.5	1.3
2a'	2.5	3	1.6	1
3'	3.8	4.4	2.1	2.3
5'	3.4	3.7	1.8; 2.2	9.6
5a'	2.9	4.1; 2.6	1.0; 1.9	1
1	1.5	1.7	1.9	1.6
4	1	1.2	2.4	3.6
5	1.1	1.2	1.9	3.8
7	1	1.0; 1.3	1.7	1.1
11; 14	1.4	1.6	2	4.4
11; 12	1.3	1.5	1.5	3.8
13	1.2	1.5	2.5	4.8

*Representative results are shown. Various analytical procedures (e.g. addition of $Cr(acac)_3$ and different detection methods including ^{13}C, ^{13}C-edited ^{1}H and DEPT) were enacted in order to find the optimal conditions. The highest background incorporation levels into the polyketide backbone were consistently observed for *S.* sp CM020.

Supplementary Table S3. Oligonucleotide primers used in this study. The 70-nt primers shown first were used for gene inactivation at the homologous recombination step, and the remaining 8 for cloning of individual genes for protein production purposes, using genomic DNA from *S.* sp. CM020 as a template. Recognition sites of the restriction endonucleases *Bgl*II and *Eco*RI used in cloning are shown in bold.

Primer	Sequence
A3fcamfor	5'-CGTATCGATATGGAGAAATCTCCGTTTGTCTCGCCGAGAGGAAGTCCCCGGTGTAGGCTGGAGCTGCTTC-3'
A3fcamrev	5'-GACCAGGGGGATCTTCCGCTCAGTCTGGGCCTGGTAGGCGGCGAAGGCCTATGGGAATTAGCCATGGTCC-3'
A6fcamfor	5'-GGACGCACCGCTGGACACCCCGAACACCCCGAGGAAAGGAGCGGCTTCGAGTGTAGGCTGGAGCTGCTTC-3'
A6fcamrev	5'- GAGCGCCTGCTGGTCACGCGGTAGGAGCCGAGCCGCACGGCCGCGCCCTGATGGGAATTAGCCATGGTCC-3'
Aln4Bfor	5'-CAG**AGATCT**CGCTACACGCTTCTCGGCAG-3'
Aln4Erev	5'-CAG**GAATTC**CTCAGGCGGCCCCGTAC-3'
Aln6Bfor	5'-CAG**AGATCT**CCGCGCAGAACGTTCGTCTC-3'
Aln6Erev	5'-CAG**GAATTC**GTCACCGCGAGCGCCTG-3'
AlnABfor	5'-CAG**AGATCT**GAACGACAGCCCGACCAGC-3'
AlnAErev	5'-CAG**GAATTC**CTCACCGCTCGGCCTGTAC-3'
AlnBBfor	5'-CAG**AGATCT**AGCGGCGCCCCCGC-3'
AlnBErev	5'-CAG**GAATTC**GTTCACGGGTGTCCGTCCAG-3'

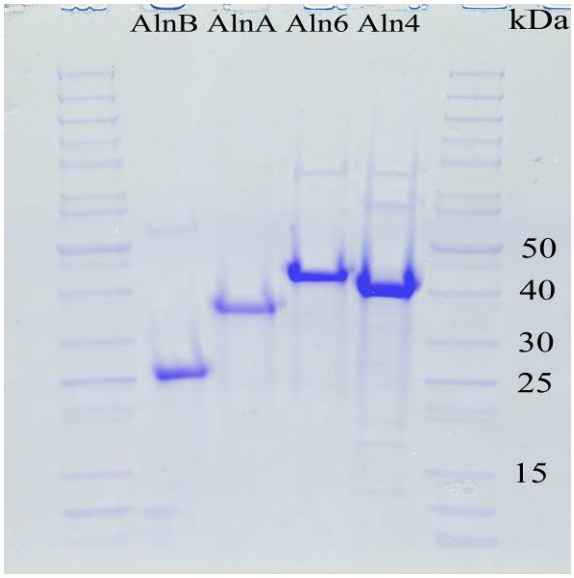

Supplementary Figure S1. Typical purity of the enzyme preparations visualized on an SDS-PAGE gel with the PageRuler unstained protein ladder (Fermentas).

S2. Supplementary Text

S2.1 NMR experimental

NMR spectra were acquired using a Bruker Avance NMR spectrometer equipped with either a 5-mm inverse or a 5-mm normal configuration probe, both with z-gradient capability, at a field strength of 11.75 T operating at 500 and 125 MHz for ^{1}H and ^{13}C nuclei, respectively, at 25 °C unless specified otherwise with samples contained in either $CDCl_3$, CD_3OD or d_6-DMSO as indicated. The chemical shifts of ^{1}H and ^{13}C nuclei are reported relative to TMS incorporated as an internal standard (δ = 0 ppm for both ^{1}H and ^{13}C) or to the solvent signals where indicated (for DMSO: δ_H = 2.49, δ_C = 39.50 ppm). General NMR experimental details for 1D ^{1}H, ^{13}C and DEPT and standard gradient-selected 2D DQF-COSY, NOESY, multiplicity-edited HSQC, HSQC-TOCSY, ^{1}H{^{13}C}-HMBC and long-range COSY spectra have been described elsewhere[31–34]. Additionally, 1,1-ADEQUATE[35] was acquired (Bruker pulse program: adeq11etgprdsp; $J_{C,H}$, 145 Hz; $J_{C,C}$, 45 Hz; sample concentration ca. 200 mg/mL) to confirm the $C_{2a'}$–$C_{3'}$ connectivity in alnumycin B (**4**). For 1D selective COSY, NOESY[36,37] (mixing time 0.5 s) and TOCSY, selective excitation was effected by excitation using a 180° 50 ms Gaussian-shaped pulse. Spin analysis was performed using Perch[38,39] iteration software for the extraction of δ_H and $J_{H,H}$. For quantitation of the ^{13}C-labeled metabolites, both ^{13}C-edited ^{1}H spectra (acquisition time, 1.64 s; post-acquisition delay time, 3.36 s; processed with 2 Hz of line broadening) and DEPT (acquisition time, 1.09 s; post-acquisition delay time, 5.0 s; variable pulse, 35°; processed with 2 Hz of line broadening) were acquired on samples containing a small amount of chromium(III) acetylacetonate as relaxation agent (half-widths of TMS signals without line broadening applied: ^{1}H, 2.0–3.0 Hz; ^{13}C, 0.7–0.8 Hz).

S2.2 Production, purification and structural elucidation of alnumycins B1 (4a) and B2 (4b)

For large scale production of **4**, 4 L of modified E1 medium with XAD-7 in Erlenmeyer flasks was inoculated with 1/100th volume of preculture of *S. albus*/pAlnuoriΔ*aln3*. As an initial step, the washed XAD-7 from 4-day old cultures was applied to an XAD-7 column in water, and secondary metabolite products were eluted with a stepwise 0–100% gradient in isopropanol. Combined fractions containing **4** were extracted with chloroform and further purified using silica gel 60 (0.040–0.063, Merck) chromatography in chloroform, and finally by preparative HPLC using

a LiChroCART 250-10 RP-18 column (10 µm, Merck) in 0.1% formic acid and a 50–100% acetonitrile gradient, resulting in ca. 97% purity (HPLC). Separation of the alnumycins B1 (**4a**, 57%) and B2 (**4b**, 43%) was achieved using the same column and a repeated isocratic run in 90:10 methanol:ammonium acetate buffer (60 mM, adjusted to pH 3.6 by addition of acetic acid), which finally resulted in a diastereomeric purity of 94% for **4a** and 92% for **4b** by NMR.

The structural elucidation of **4a** and **4b** followed from the molecular formula of $C_{22}H_{22}O_8$ provided by EI^+-HR-MS (*m/z* observed 414.1328 amu, calculated 414.1315 amu). High resolution EI-MS data for **4** was measured using a ZABSpec mass spectrometer (VG Analytical) with settings of 70 eV ionization energy, 433 K source temperature, 8 kV accelerating voltage and 200 mA trap current. The determination of an intact prealnumycin moiety in each case was inferred by the observation of (a) a chromophore in UV-vis spectroscopy pertaining to such and (b) the straightforward 2D spectra-based recognition and assignment of the ^1H and ^{13}C NMR signals (Supplementary Table S4) for a prealnumycin moiety substituted at C-8, which was consistent with previous observations[12,13,40] and other compounds in this work.

Supplementary Table S4. ^{1}H and ^{13}C NMR assignments of alnumycin B1 (**4a**) and alnumycin B2 (**4b**) in CD_3OD at 25 °C. The chemical shifts of the nuclei are reported relative to TMS as an internal standard (δ = 0 ppm for ^{1}H and ^{13}C).

	alnumycin B1 (**4a**)				alnumycin B2 (**4b**)			
pos.	δ/ppm		mult.	$J(^{1}H,^{1}H)$/Hz	δ/ppm		mult.	$J(^{1}H,^{1}H)$/Hz
	^{13}C/ppm	^{1}H/ppm		(spin partner)	^{13}C/ppm	^{1}H/ppm		(spin partner)
1	73.02	5.652	app dd	9.33 (H-11a), 3.56 (H-11b)	73.02	5.651	app dd	9.33 (H-11a), 3.53 (H-11b)
3	158.66				158.67			
4	100.02	5.608	qt	−0.87 (H-14)	100.04	5.609	qtd	−0.85 (H-14), −0.32 (H-5)
4a	139.78				139.82			
5	114.44	7.135	br s		114.52	7.141	br s	−0.32 (H-4)
5a	131.39				131.43			
6	184.72				184.71			
7	134.73	6.972	d	−0.93 (H-1')	135.35	7.136	d	−0.94 (H-1')
8	144.27				143.84			
9	187.74				187.69			
9a	113.02				112.93			
10	157.14	12.156	s		157.12	12.142	s	
10a	122.49				122.41			
11	34.86	a, 1.99	m	9.33 (H-1)	34.87	a, 2.00	m	9.33 (H-1)
		b, 1.53	m	3.56 (H-1)		b, 1.53	m	3.53 (H-1)
12	18.119	1.55	m		18.123	1.55	m	
		1.49	m			1.49	m	
13	13.787	0.959	app t	7.12 (H-12 × 2)	13.789	0.959	app t	7.13 (H-12 × 2)
14	20.437	1.965	d	−0.87 (H-4)	20.435	1.966	d	−0.85 (H-4)
1'	99.51	β, 6.178	d	−0.93 (H-7)	99.18	α, 5.985	d	−0.94 (H-7)
2a'	84.88	4.725	d	5.54 (H-5a')	85.92	4.741	d	6.10 (H-5a')
3'	101.30	5.596	br s	−0.52 (H-5a'), −0.68 (H-5'β),	101.23	5.529	br s	−0.49 (H-5a')
5'	72.11	β, 4.213	ho ddd	−10.80 (H-5'α), −0.68 (H-3'),	71.48	4.142a	d	2.00 (H-5a')
				0.65 (H-5a')		4.142b	d	2.08 (H-5a')
		α, 4.187	br ho dd	−10.80 (H-5'β), 3.92 (H-5a')				
5a'	80.53	5.011	ho dddd	5.54 (H-2a'), 3.92 (H-5'α),	81.34	4.987	dtd	6.10 (H-2a'), 2.00 (H-5'a),
				0.65 (H-5'β), −0.52 (H-3')				2.08 (H-5'b), −0.49 (H-3')

Legend: app, apparent; br, broad or broadened; d, doublet; ho, higher order; m, multiplet; qt, quartet; s, singlet; t, triplet.

For the sidechain structure, the presence of a *cis*-bicyclo[3.3.0]-2',4',6'-trioxaoctan-3'β-ol moiety (i.e. a "2,6-dioxolane" sub-structure is present within) was implied by the similarity of the sub-spectra to that for 2,3-*O*-ethylidene-β-D-erythrofuranose[41] (or otherwise *cis*-bicyclo[3.3.0]-1,3,5-trioxaoctan-4β-ol). The attachment of this group to C-8 of the prealnumycin skeleton and the attachment of the prealnumycin moiety to the dioxolane carbon in the sidechain were evident from long-range COSY and HMBC correlations between appropriate nuclei. Intriguingly, the coupling between H-2a' and H-3' ($J_{H2a',H3'}$) in both isomers **4a** and **4b** was only ca. 0 Hz in size, thus data on this connectivity was not forthcoming by COSY in either case and the evidence needed to confirm the $C_{2a'}$–$C_{3'}$ connection in both **4a** and **4b** to secure the gross structures was ultimately only provided by 1,1-ADEQUATE[35]. This small size for $J_{H2a',H3'}$ implies that the torsion angle between them must be ca. 90º, and since this was the case for both isomers, the case of a pair of C-3' epimers constituting **4a** and **4b** is thereby excluded. In actual fact, the C-3' epimers of **4a** and **4b** are energetically disfavored due to steric hindrance with the fused dioxolane ring[41].

Henceforth, the supposition then followed that since the largest chemical shift differences between the isomers were for nuclei proximal to C-1', **4a** and **4b** thus constitute a C-1' epimeric pair. To confirm this supposition, simplified models to facilitate rapid computations (based on the premise that the planar prealnumycin section is unlikely to affect the *cis*-bicyclo[3.3.0]-2',4',6'-trioxaoctan-3'β-ol moiety to any great extent) were constructed for **4a** and **4b** (Supplementary Fig. S2). For these models, a conformational search was performed using the molecular dynamic method implemented in *HyperChem 7.5*[42]. The lowest energy structures thus obtained also seemed the most promising based on the torsion angles between *vicinal* Hs and internuclear H, H distances ($r_{H,H}$) in comparison to the NMR results. The global minimum conformations were then further optimized using density functional theory implemented in *Gaussian03*[43] at the B3LYP/6-31G(d,p) level of

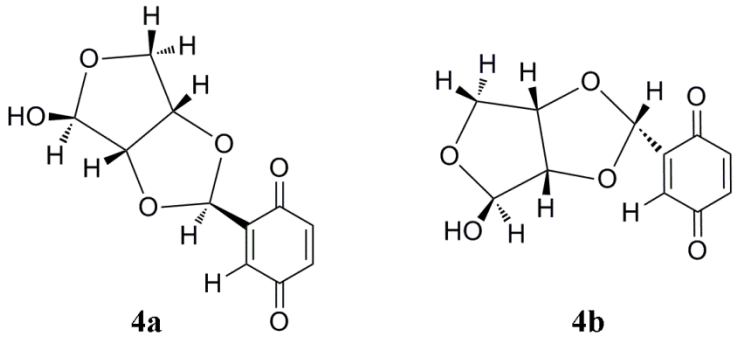

Supplementary Figure S2. The structures of the model compounds for alnumycins B1 (**4a**) and B2 (**4b**).

theory. Scalar coupling constants (J) were calculated for the final optimized structures at the same level of theory. Supplementary Table S5 shows selected calculated data together with the corresponding experimental results whilst Cartesian coordinates and depictions of the optimized structures are presented in Supplementary Fig.s S3 and S4. Since the calculated data of the optimized structures are in good agreement with the experimental NMR results with respect to various $J_{H,H}$ and $r_{H,H}$ values, the models therefore describe accurately the three-dimensional structure of the *cis*-bicyclo[3.3.0]-2',4',6'-trioxaoctan-3'β-ol moieties in **4a** and **4b**.

Supplementary Table S5. Comparison between selected experimental NMR data for alnumycin B1 (**4a**) and B2 (**4b**) and calculated data for optimized model structure.

^{1}H nuclei	(**4a**)		(**4b**)	
	r (calculated) / Å	NOE contact	*r* (calculated) / Å	NOE contact
H-1', H-7	2.3	*s*	3.6	*w*
H-1', H-2a'	4.0	–	3.5	*s*
H-1', H-3'	3.8	*s*	4.6	–
H-1', H-5a'	3.9	–	3.7	*s*
H-7, H-2a'	5.5	–	4.2	*w*
H-7, H-3'	5.9	–	2.7	*s*
	J (calculated) / Hz	*J* (observed) / Hz	*J* (calculated) / Hz	*J* (observed) / Hz
H-1', H-7	0.8	0.9	−1.4	0.8
H-2a', H-3'	−0.3	0	−0.2	0
H-2a', H-5a'	5.8	5.7	5.8	6.1

Legend: *s*, strong; *w*, weak; –, NOE contact not observed.

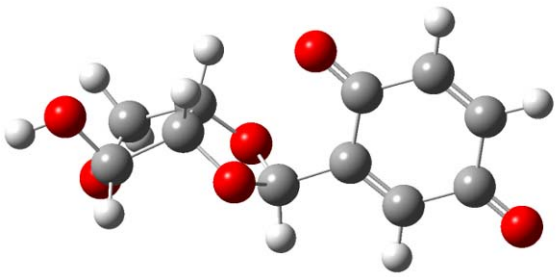

Supplementary Figure S3. The calculated structure of the model structure for alnumycin B1 (**4a**). Cartesian coordinates:

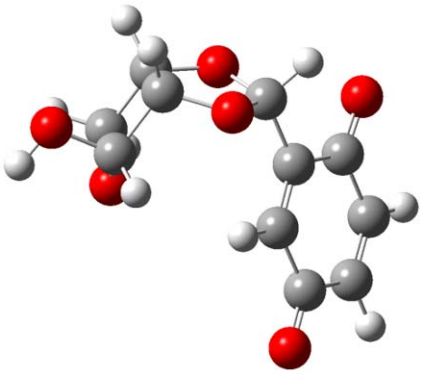

Supplementary Figure S4. The calculated structure of the model structure for alnumycin B2 (**4b**). Cartesian coordinates:

Of note, the relative dispositions of H-2a' and H-5a' in relation to the dioxolane ring in both **4a** and **4b** were expected to be *cis* since this relationship is provided by D-ribose from whence the C_4 segment in **4a** and **4b** originates. In concert with this expectation of a *cis* configuration, scalar couplings of 5.7 and 6.1 Hz for the $J_{H2a',H5a'}$ couplings were extracted, which were also well in agreement with the two calculated values of 5.8 Hz (Supplementary Table S5). This origin of the C_4 segment also then provides the absolute stereochemistry for C-2a' and C-5a' in **4a** and **4b**, viz. *RR*. Thus, based on these results, it was deduced that **4a** and **4b** constitute a pair of C-1' epimers for the structures indicated and that the major isomer **4a** has H-1' *trans* to H-2a' and H-5a'.

S2.3 Production, purification and structural elucidation of alnumycins C1 (anhydroexfoliamycin[44], 5a), C2 (5b) and D (6)

For large scale production of **5** and **6**, the mutant strain *S. albus*/pAlnuoriΔind + pIJa7ABK118R, for which the production levels of **5** and **6** were comparable to *S. albus*/pAlnuoriΔ*aln6*, was similarly cultivated for 5 days. The strain *S. albus*/pAlnuoriΔind + pIJa7ABK118R contains the previously described cosmid pAlnuoriΔind (14), which contains the alnumycin gene cluster from which the genes *alnA* and *alnB* have been inactivated, and a complementation plasmid pIJa7ABK118R, which contains native *alnA* and *alnB* with a K118R mutation. The strain presumably produces **5** and **6** due to a metabolic-flux phenomenon (Oja et al., unpublished results).

The preparative-scale purification of alnumycins C (**5**) and D (**6**) was attained via column chromatography using XAD-7 resin eluted with water and a 5–90% isopropanol gradient followed by a second column using silica gel eluted with $CHCl_3$ and a 0–15% methanol gradient and then finally preparative HPLC using a SunFire Prep C18 column (5 μm, Waters) eluted with 80% methanol and 20% 60 mM aqueous ammonium acetate at pH 3.6. This yielded **5** (93% pure by HPLC) whilst **6** (ca. 90% pure by HPLC) was only obtained sufficiently pure after additional preparative HPLC using the SunFire Prep C18 column eluted with 20 mM aqueous ammonium acetate and a 55–100% acetonitrile gradient. The separation of the stereoisomeric alnumycins C1 (**5a**) and C2 (**5b**) was achieved via a second silica column eluted with 7:3 hexane:isopropanol and a final purification by preparative HPLC eluting with 20 mM aqueous ammonium acetate and a 55–100% acetonitrile gradient resulting in higher than 98% diastereomeric purity for both **5a** and **5b** by NMR.

The structural elucidations of **5a**, **5b** and **6** followed from ESI^--HR-MS which provided accurate masses of 415.1394 for **5** and 415.1399 for **6** for the M − 1 ions alluding to a molecular formula of $C_{22}H_{24}O_8$ in each case (calculated for the M − 1 ions, 415.1398 amu). HPLC-ESI-MS were acquired using a MicrOTOF-Q mass spectrometer (Bruker) with settings of 4 kV capillary voltage, 573 K dry heater temperature and 1.6 bar nebulizer pressure and an Agilent Technologies 1200 Series HPLC system equipped with a diode array detector and a SunFire C18 column (3.5 μm, Waters) eluted with 0.1% aqueous formic acid and a 15–100% acetonitrile gradient. The determination of an intact prealnumycin moiety in each case was inferred by the observation of (a) a chromophore in UV-vis spectroscopy pertaining to such and (b) the straightforward 2D spectra-based recognition and assignment of the ^1H and ^{13}C NMR signals (Supplementary Table S6) for a prealnumycin moiety substituted at C-8 and which was consistent with previous observations[12, 13, 40] and other compounds in this work. For the sidechain structure, by COSY (with support from DEPT and HSQC spectra revealing four methines and one methylene in a region typical for singly oxygenated resonances), a pentose-type chain was readily mapped out for each of **5** and **6**, which thus completed the sidechain constitution taking into account the molecular formula, with the important result that the connection between the prealnumycin moiety and the ribose unit must be via a C–C bond rather than a typical glycosidic ethereal –O– bond.

Supplementary Table S6. ^{1}H and ^{13}C chemical shifts and the most important NOE signals for alnumycin C1 (anhydroexfoliamycin[44], **5a**), C2 (**5b**) and D (**6**) in CD_3OD at 25 °C. The chemical shifts of ^{1}H and ^{13}C nuclei are reported relative to TMS as an internal standard (δ = 0 ppm for both ^{1}H and ^{13}C).

	alnumycin C1 (**5a**)				alnumycin C2 (**5b**)			
pos.	δ/ppm		mult.	$J_{(H,H)}$/Hz	δ/ppm		mult.	$J_{(H,H)}$/Hz
	^{13}C/ppm	^{1}H		(spin partner)	^{13}C/ppm	^{1}H/ppm		(spin partner)
1	73.04	5.658	app dd	9.33 (H-11a), 3.52 (H-11b)	73.00	5.646	app dd	9.35 (H-11a), 3.53 (H-11b)
3	159.39				158.57			
4	100.17	5.625	qt	−0.87 (H-14)	100.11	5.613	qt	−0.85 (H-14)
4a	140.58				139.80			
5	115.14	7.159	s		114.58	7.152	s	
5a	131.44				131.62			
6	184.19				184.29			
7	133.99	7.017	d	−1.86 (H-1')	135.11	7.029	d	−1.93 (H-1')
8	149.01				147.80			
9	189.42				188.61			
9a	112.95				112.95			
10	157.49	11.986	s		157.09	12.176	s	
10a	122.02				122.03			
11	34.89	a, 2.00	m		34.97	a, 2.00	m	
		b, 1.53	m			b, 1.52	m	
12	18.11	1.56	m		18.14	1.54	m	
		1.49	m			1.49	m	
13	13.78	0.968	app t	7.12 (H-12 × 2)	13.80	0.965	app t	7.11 (H-12 × 2)
14	20.51	1.980	d	−0.87 (H-4)	20.45	1.968	d	−0.85 (H-4)
1'	80.45	4.904	ddd	6.39 (H-2'), −1.86 (H-7), −0.54 (H-3')	78.22	5.213	dd	4.14 (H-2'), −1.93 (H-7)
2'	75.34	4.111	ho t	6.39 (H-1'), 5.94 (H-3')	73.14	4.667	~t	4.79 (H-3'), 4.14 (H-1')
3'	72.27	4.184	ho dd	5.94 (H-2'), 4.45 (H-4'), −0.54 (H-1')	72.44	4.422	ho dd	8.04 (H-4'), 4.79 (H-2')
4'	84.91	4.150	ho td	4.45 (H-3'), 4.28 (H-5'$_{proS}$), 3.24 (H-5'$_{proR}$)	81.46	3.977	ho m	8.04 (H-3'), 3.75 (H-5'$_{proS}$), 3.33 (H-5'$_{proR}$)
5'$_{proR}$	62.92	3.935	$d_{AB}d$	−11.94 (H-5'$_{proS}$), 3.24 (H-4'),	62.01	3.981	ho m	−12.01 (H-5'$_{proS}$), 3.33 (H-4'),
5'$_{proS}$		3.798	$d_{AB}d$	−11.94 (H-5'$_{proR}$), 4.28 (H-4')		3.802	ho m	−12.01 (H-5'$_{proR}$), 3.75 (H-4')

Supplementary Table S6. (Continued)

	alnumycin D (**6**)			
pos.	δ/ppm		mult.	$J(^1H,^1H)$/Hz
	^{13}C/ppm	^1H/ppm		(spin partner)
1	73.06	5.643	app dd	9.39 (H-11a), 3.50 (H-11b)
3	158.94			
4	100.13	5.612	qt	−0.90 (H-14)
4a	140.15			
5	114.73	7.136	s	
5a	131.33			
6	184.26			
7	135.57	6.985	d	−1.18 (H-1')
8	149.82			
9	189.09			
9a	112.88			
10	157.33	12.120	s	
10a	122.11			
11	34.86	a, 2.01	m	9.39 (H-1)
		b, 1.52	m	3.50 (H-1)
12	18.15	1.55	m	
		1.48	m	
13	13.79	0.964	app t	7.13 (H-12 × 2)
14	20.48	1.970	d	−0.90 (H-4)
1'	69.59	4.751	~dt	9.32 (H-2'), −1.18 (H-7), 0.75 (H-3')
2'	73.86	3.488	dd	9.32 (H-1'), 2.72 (H-3')
3'	70.99	4.251	br t	3.09 (H-4'), 2.72 (H-2'), 0.75 (H-1')
4'	66.92	3.884	ho m	10.91 (H-5'α), 5.73 (H-5'β), 3.09 (H-3')
5'α	66.12	3.598	ho m	10.91 (H-4'), −10.85 (H-5'β)
5'β		3.897	ho m	−10.85 (H-5'α), 5.73 (H-4')

Legend: app, apparent; ho, higher order; s, singlet; d, doublet; t, triplet; qt, quartet; m, multiplet; dAB, doublet with higher order perturbation of the intensities.

^{1}H and COSY analysis of the compounds in d_6-DMSO or mixtures thereof then readily identified **5a** and **5b** as furanose forms and **6** as a pyranose form as indicated by the positioning of the free glycosidic OHs (confirmed as exchangeable by saturation transfer) based on the *vicinal* ^{1}H,^{1}H scalar coupling constants ($J_{H,H}$) and COSY correlations (for **6**, three doublets for the hydroxyl protons were observed which were coupled to H-2', H-3' and H-4'; for **5a** and **5b**, two doublets and one triplet were observed for the hydroxyl protons which were coupled to H-2', H-3' and H-5', respectively). The attachment of the ribose unit to C-8 of the prealnumycin skeleton and the attachment of the prealnumycin moiety to the ribose C-1 carbon in each case was evident from long-range COSY and HMBC correlations with confirmation in the latter experiments that the connection extended over a C–C bond rather than a C–O–C linkage. Pertinent NOE contacts and the magnitude of the various $J_{H,H}$s extracted with Perch[38,39] then completed the structural assignment identifying **5a** and **6** as β anomers and **5b** as an α anomer. The NOE contacts also supported the ring configurations in the former pair.

The relative stereochemistries of the sugar ring C-2', C-3' and C-4' stereogenic centers in **5** and **6**, with determination based on NOE contacts and $J_{H,H}$s, in **5** and **6** are the same as that for D-ribose, and since labeling studies indicate that D-ribose is utilized for the production of alnumycins B1 (**4a**) and B2 (**4b**) by the strain and furthermore, since **4** was synthesized *in vitro* from **5**, it then follows that the absolute configurations of the sugar rings are as depicted (*R*2',*R*3',*R*4' in each case).

Additionally, the $J_{H,H}$s and NOEs also indicated a $^4C_1$ conformation (with respect to conventional Haworth representation) for the pyranose ring in **6**. The assignments of the H-5's (denoted as *proR* and *proS* for **5** whilst denoted as α and β with respect to Haworth representation for **6**) were effected by evaluation of NOE contacts and scalar coupling constants in **5** and **6**, and for **5**, the assignments were in accordance with literature[45,46]. Of particular note, only one stereoisomer, the β anomer, was observed for the pyranose form **6** in contrast to the similarly ribose-substituted pair **5a** and **5b**, and correspondingly also for **4**.

Finally, **5a** has been reported previously[44,47], where it was denoted as anhydroexfoliamycin, and the NMR data reported herein is consistent with that account. The authors were cautious about assuming the incorporation of D-ribose, which is now confirmed.

S2.4 Purification and structural elucidation of alnumycin S (7)

For preparative production of alnumycin S (**7**), a total of 25 mL of a reaction mixture consisting of 3 mM NADPH, 0.5 mM alnumycin B (**4**) and 2 μM Aln4 was divided into three tubes

and incubated under aerobic conditions for 1 h at 288 K and stirring at 60 rpm. After incubation, each reaction was extracted with 4 × 1 volume of $CHCl_3$. The combined extracts in acetonitrile were then subjected to preparative HPLC using a SunFire Prep C18 (5 μm, Waters) column eluted with 20 mM aqueous ammonium acetate and a 55–100% acetonitrile gradient to obtain **7**, ca. 90% pure by HPLC.

The structural elucidation of **7** followed from ESI^--HR-MS which provided an accurate mass of 415.1394 amu for the M − 1 ion alluding to a molecular formula of $C_{22}H_{24}O_8$ (calculated for the M − 1 ion, 415.1398 amu). The determination of an intact prealnumycin moiety was inferred by the observation of (a) a chromophore in UV-vis spectroscopy pertaining to such and (b) the protons and eight proton-bearing carbons (Supplementary Table S7) which were consistent with regards to both chemical shift and multiplicity to previous observations of the prealnumycin moiety (other compounds in this work and refs. 12, 13 and 40; due to limited sample amount, direct observation of carbon was not possible and only indirect observation of the proton-bearing carbons was amenable via multiplicity edited HSQC). This left only the structure of the sidechain to be established.

Since the M.W. of **7** was only two mass units greater than **4** from which it was derived, it was assumed that the position 3' of the hemiacetal unit in **4** had been reduced to a primary alcohol to yield **7** (Fig. 1) containing a di(hydroxylmethyl)-substituted dioxolane unit. This was substantiated by the continued presence of the deshielded dioxolane H-1' and C-1' nuclei evident in the ^1H and ^{13}C NMR, respectively, and the near-symmetric environment in the new unit (differentiated only by the distant C-1 stereogenic center) giving rise to essentially chemically equivalent $–CHCH_2OH$ segments with signals at appropriate resonances in both the ^1H and ^{13}C NMR. Perch[38,39] spin simulation and iteration of the complex ^1H sub-spectrum for the $–CHCH_2OH$ segments provided support for the proposed constituent of two adjacent $–CHCH_2OH$ segments by sufficient reproduction of the experimental sub-spectrum and the appropriateness of the extracted scalar couplings. The attachment of the dioxolane to C-8 of the prealnumycin skeleton and the attachment of the prealnumycin moiety to the dioxolane carbon in the sidechain was evident by the long-range coupling between H-7 and H-1'.

Supplementary Table S7. Partial ^{1}H and ^{13}C NMR assignments of alnumycin S (**7**) in $CDCl_3$ at 25 °C. The chemical shifts of ^{1}H and ^{13}C nuclei are reported relative to TMS as an internal standard (δ = 0 ppm for both ^{1}H and ^{13}C).

alnumycin S (**7**)				
pos.	δ/ppm		mult.	$J_{(H,H)}$/Hz (spin partner)
	$^{13}C^{a}$	$^{1}H^{b}$		
1	73.1	5.658	app dd	9.29 (H-11a); 3.53 (H-11b)
3	no	–		
4	100.0	5.614	qt	0.90 (H-14)
4a	no	–		
5	114.7	7.149	br s	
5a	no	–		
6	no	–		
7	135.7	7.071	d	0.90 (H-1')
8	no	–		
9	no	–		
9a	no	–		
10	no	12.148	s	
10a	no	–		
11	35.0	2.04, 1.51	m	
12	18.3	1.55, 1.48	m	
13	13.8	0.960	app t	7.08 (2 × H-12)
14	20.3	1.970	d	0.90 (H-4)
1'	97.4	5.945	d	0.90 (H-7)
3'/''	78.3	4.41	ho m	6.5 (H-3''); 5.9 (H-4a'); 4.3 (H-4b')
4'/''	60.5	3.93a, 3.88b	ho m	−12.1 (J_{gem}); 5.9 (a, H-3'); 4.3 (b, H-3')

Legend: app, apparent; br, broad or broadened; d, doublet; ho, higher order; m, multiplet; no, not observed; qt, quartet; s, singlet; t, triplet. [a] Proton-bearing carbon δs measured indirectly (they are thus reported to only one decimal place to reflect the lower acquired resolution) from an HSQC spectrum with editing, all correlations were to methines except for C-4'/4'' which was to a methylene carbon. The reduced resolution precluded any chance to observe distinctions between C-3' and 3'' and between C-4' and 4''. [b] Data extracted using Perch for signals other than singlets and the 1–11–12–13 spin system. The shifts and couplings for the non-equivalent H-3'/3'' and H-4'/4'' pairs could not be disentangled and are reported as one set of signals representing a $-CHCH_2OH$ segment; the complexity and breadth of the multiplet lines also precluded more precise evaluation of the shifts and couplings and this reduced reliability in their value is reflected by reporting them to only two and one decimal places, respectively.

The relative stereochemistries of C-3' and C-3'' (now a *meso* pair of stereogenic centers) in relation to the ring were expected to be the same as that present in alnumycin B, viz. they should be *cis* to each other with respect to the dioxolane ring, and the same relationship is even provided by D-

ribose for whence the complete dioxolane unit of **4** has been shown to originate from by labeling studies and *in vitro* enzymatic assays. In concert with this expectation of a *cis* configuration was an extracted scalar coupling of 6.5 Hz for $J_{H3',H3''}$. Significantly, the ^{1}H NMR spectrum of **7** pertaining to the sidechain is totally inconsistent with that of *trans*-4,5-di(hydroxymethyl)-1,3-dioxolane[48,49]. As a result of reduction to identical substituents, C-3' and C-3'' now represent a *meso* pair of stereogenic centers, rendering moot the assignment of absolute configuration for these stereogenic centers. The *cis* relationship between H-1' and H-3'/3'' was determined by the observation of strong NOE contacts between the two sets of nuclei.

S2.5 Incorporation experiments with ^{13}C-labeled D-ribose-5-phosphate

Both [U-^{13}C] and [5-^{13}C] D-ribose, together with unlabeled D-ribose as a control, were each dissolved in 100 µL of sterile water and fed separately in 4 equal batches over the course of 24–48 h from inoculation to 20 mL cultures of *S.* sp. CM020 to a total concentration of 0.06% (w/v) in parallel with unlabeled sodium pyruvate (total 0.2%, w/v) to reduce scrambling of the labeled D-ribose via glycolysis. XAD-7 taken from 3-day old cultures was extracted with isopropanol and the extract applied to an isocratic silica column eluted with 7:3 hexane:isopropanol to obtain labeled **1** and **4**. Labeled **4** was also obtained by the feeding of [U-^{13}C] D-ribose to *S. albus*/pAlnuorid*aln3* in 5 batches over the course of 36–72 h from inoculation followed by the extraction of 4-day old cultures.

Similarly, [U-^{13}C] and [5-^{13}C] D-ribose together with unlabeled D-ribose were fed to *S. albus*/pAlnuori in **7** equal batches over the course of 24–72 h from inoculation. Prior to NMR analysis, fractions containing **1** or **4** were further purified by preparative HPLC equipped with a LiChroCART 250-10 RP-18 column (10 µm, Merck) eluted with 20 mM aqueous ammonium acetate and a 55–100% acetonitrile gradient.

Supplementary references

(31) Mäki, J.; Tähtinen, P.; Kronberg, L.; Klika, K. D. *J. Phys. Org. Chem.* **2005**, *18*, 240.

(32) Virta, P.; Koch, A.; Roslund, M. U.; Mattjus, P.; Kleinpeter, E.; Kronberg, L.; Sjöholm, R.; Klika, K. D. *Org. Biomol. Chem.* **2005**, *3*, 2924.

(33) Klika, K. D.; Bernát, J.; Imrich, J.; Chomča, I.; Sillanpää, R.; Pihlaja, K. *J. Org. Chem.* **2001**, *66*, 4416.

(34) Balentová, E.; Imrich, J.; Bernát, J.; Suchá, L.; Vilková, M.; Prónayová, N.; Kristian, P.; Pihlaja, K.; Klika, K. D. *J. Heterocycl. Chem.* **2006**, *43*, 645.

(35) Köck, M.; Kerssebaum, R.; Bermel, W. *Magn. Reson. Chem.* **2003**, *41*, 65.

(36) Stonehouse, J.; Adell, P.; Keeler, J.; Shaka, A. J. *J. Am. Chem. Soc.* **1994**, *116*, 6037.

(37) Stott, K.; Stonehouse, J.; Keeler, J.; Hwang, T. L.; Shaka, A. J. *J. Am. Chem. Soc.* **1995**, *117*, 4199.

(38) Peak Research NMR Software; Perch Solutions, Ltd.: Kuopio, Finland, 2003 (website: http://www.perchsolutions.com).

(39) Laatikainen, R.; Niemitz, M.; Weber, U.; Sundelin, J.; Hassinen, T.; Vepsäläinen, J. *J. Magn. Reson. Ser. A* **1996**, *120*, 1.

(40) Tatsuta, K.; Tokishita, S.; Fukuda, T.; Kano, T.; Komiya, T.; Hosokawa, S. *Tetrahedron Lett.* **2011**, *52*, 983.

(41) Van Cleve, J. W.; Rist, C. E. *Carbohydr. Res*. **1967**, *4*, 82.

(42) *HyperChem Release 7.5* for Windows, Hypercube Inc.

(43) Gaussian 03, Revision E.01, Frisch, M. J. *et al*., *Gaussian*, Inc., Wallingford CT, 2004.

(44) Potterat, O.; Zähner, H.; Volkmann, C.; Zeeck, A. *J. Antibiot.* **1993**, *46*, 346.

(45) Plavec, J.; Tong, W.; Chattopadhyaya, J. *J. Am. Chem. Soc.* **1993**, *115*, 9734.

(46) Olsen, R.; Backman, J.; Molander, P.; Klika, K. D.; Kronberg, L. *Eur. J. Org. Chem.* **2007**, 4011.

(47) Volkmann, C.; Zeeck, A.; Potterat, O.; Zähner, H.; Bohnen, F.-M.; Herbst-Irmer, R. *J. Antibiot.* **1995**, *48*, 431.

(48) Gras, J.-L.; Pellissier, H.; Nougier, R. *J. Org. Chem.* **1989**, *54*, 5675.

(49) Dulphy, H.; Gras, J.-L.; Lejon, T. *Tetrahedron* **1996**, *52*, 8517.